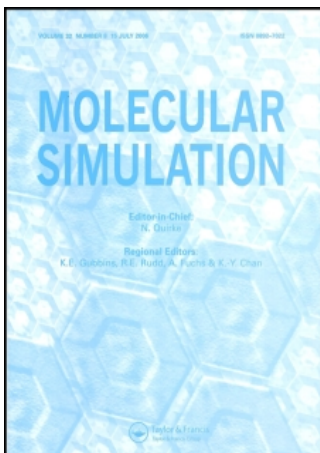


This article was downloaded by:[Universiteit Gent]
On: 23 August 2007
Access Details: [subscription number 781058445]
Publisher: Taylor & Francis
Informa Ltd Registered in England and Wales Registered Number: 1072954
Registered office: Mortimer House, 37-41 Mortimer Street, London W1T 3JH, UK



Molecular Simulation

Publication details, including instructions for authors and subscription information:
<http://www.informaworld.com/smpp/title~content=t713644482>

Modeling elementary reactions in coke formation from first principles

Online Publication Date: 01 August 2007

To cite this Article: Van Speybroeck, V., Hemelsoet, K., Minner, B., Marin, G. B. and Waroquier, M. (2007) 'Modeling elementary reactions in coke formation from first principles', Molecular Simulation, 33:9, 879 - 887

To link to this article: DOI: 10.1080/08927020701308315

URL: <http://dx.doi.org/10.1080/08927020701308315>

PLEASE SCROLL DOWN FOR ARTICLE

Full terms and conditions of use: <http://www.informaworld.com/terms-and-conditions-of-access.pdf>

This article maybe used for research, teaching and private study purposes. Any substantial or systematic reproduction, re-distribution, re-selling, loan or sub-licensing, systematic supply or distribution in any form to anyone is expressly forbidden.

The publisher does not give any warranty express or implied or make any representation that the contents will be complete or accurate or up to date. The accuracy of any instructions, formulae and drug doses should be independently verified with primary sources. The publisher shall not be liable for any loss, actions, claims, proceedings, demand or costs or damages whatsoever or howsoever caused arising directly or indirectly in connection with or arising out of the use of this material.

© Taylor and Francis 2007

Modeling elementary reactions in coke formation from first principles

V. VAN SPEYBROECK^{†*}, K. HEMELSOET[†], B. MINNER[†], G. B. MARIN[‡] and M. WAROQUIER[†]

[†]Center for Molecular Modeling, Ghent University, Proeftuinstraat 86, 9000 Ghent, Belgium

[‡]Laboratorium voor Petrochemische Techniek, Ghent University, Krijgslaan 281-S5, 9000 Ghent, Belgium

(Received December 2006; in final form February 2007)

Theoretical calculations are presented on elementary reactions which are important during coke formation in a thermal cracking unit. This process is known to proceed through a free radical chain mechanism. The elementary reaction steps that lead to the growth of the coke surface can be divided into five classes of reversible reactions: hydrogen abstraction, substitution, gas phase olefin addition to radical surface species, gas phase radical addition to olefinic bonds and cyclization. To identify the elementary reaction classes that determine the coking rate, all microscopic routes that start from benzene and lead to naphthalene have been investigated. It is found that initial creation of surface radicals, either by hydrogen abstraction or substitution and subsequent hydrogen abstractions, determines the global coking rate. The influence of the local polyaromatic structure on the kinetics of the hydrogen abstraction reactions is determined by performing calculations on a large set of polyaromatic hydrocarbons (PAHs). On basis of the BDE values six types of possible reactive sites at the coke surface can be distinguished. For the initial hydrogen abstraction the local polyaromatic structure strongly influences the reaction kinetics and abstraction is preferred from less congested sites of the polyaromatic.

Keywords: Radical reactions; Hydrogen abstraction; Density functional calculations; Polyaromatic hydrocarbons; Bond dissociation enthalpy; Coke

1. Introduction

Thermal cracking of hydrocarbons is the simplest and oldest method for petroleum refinery processes and is considered as the main process for the production of light olefins such as ethene. The thermal cracking of hydrocarbons is known to proceed through a free radical chain mechanism. Radicals are mainly formed via C–C bond breaking and propagation occurs through abstraction and β -scission reactions. Decomposition of radicals by β -scission results in the desired gas-phase olefins. During this process, highly undesirable carbon-rich products are formed on the inner walls of the reactor giving rise to the formation of a coke layer. This coke layer has a negative influence on the efficiency of the cracking unit. The process of coke formation is a complex phenomenon [1–3]. Initially, coke is formed by a heterogeneous catalytic mechanism in which the properties of the inner tube skin play an important role. Once the metal surface is covered with coke the catalytic activity of the metal particles diminishes and a heterogeneous non-catalytic

mechanism becomes important. The coke layer thus formed has a polynuclear aromatic character. Usually, one focuses on the second process since the period of catalytic coke formation is very small with respect to the total run length. In today's operation of a plant simulation models play a very important role. Recently, a coking model based on elementary reactions was developed at the Laboratorium voor Petrochemische Techniek [3,4]. In view of the fundamental nature of the elementary steps considered such a model is of general applicability. One of the main challenges in the development of an accurate and broadly applicable model is the assignment of rate coefficients for individual reactions occurring in the reaction network. The fundamental nature of the elementary steps considered allows the use of theoretical calculations to provide kinetic and thermodynamic data and to obtain microscopic insight in the basic reaction steps of the coke formation model. The elementary reaction steps that lead to incorporation of carbon atoms and growth of the coke surface can be divided in five classes of reversible reactions (figure 1):

*Corresponding author. Email: veronique.vanspeybroeck@ugent.be

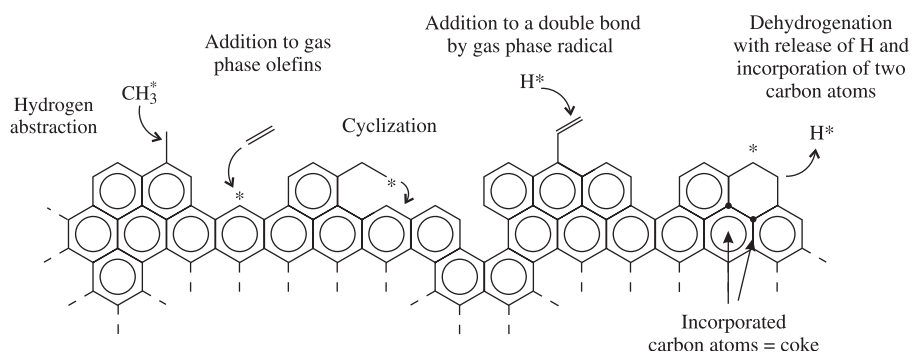


Figure 1. Radical elementary reaction steps leading to coke growth.

- i) Hydrogen abstraction reactions by gas phase radicals and reverse reactions.
- ii) Substitution reactions by radicals at the coke surface and reverse reactions.
- iii) Addition reactions of radical surface species to gas phase olefins and the inverse β -scission of a radical surface species in smaller surface species and gas phase olefins.
- iv) Addition reactions of gas phase radicals to olefinic bonds in a surface species and the inverse decomposition of radical surface species to gas phase radicals and olefinic surface species.
- v) Cyclization of radical surface species and decyclization.

Due to the increasing capabilities of computing power and optimization of numerical models it is now possible to perform high level *ab initio* calculations on systems of industrial importance. Kinetic parameters, such as the preexponential factor and activation energy, can be obtained by means of transition state theory (TST). The microscopic quantities are obtained by means of *ab initio* calculations. In this work preference has been given to Density Functional Theory calculations, since this approach is computationally attractive for the larger structures that are involved. This approach has been successfully applied to a variety of important chemical reactions. In the first part of this paper, microscopic routes starting from benzene leading to the formation of naphthalene are investigated with the aim to obtain insight into the elementary reaction classes that determine the rate of coke formation. In the second part of the paper, larger polyaromatic clusters are considered in order to determine the influence of the coke matrix on the kinetics of the elementary reactions.

2. Methodology

All calculations were performed using the Gaussian 03 software package [5]. Geometries were optimized at the B3-LYP level of theory, in conjunction with the 6-311G(d,p) basis set [6,7]. A previous study on the hydrogen-abstraction reaction from benzene with the methyl radical showed the limited influence of the

level of theory on the optimized geometries [8]. Other studies on related radical reactions also reported that B3-LYP gives a reliable and quantitatively good description of geometries [9–11]. Frequencies were computed at the same level of theory as the geometry optimizations to provide zero-point vibrational energies (ZPVEs) and thermal corrections to the enthalpy, and to confirm the nature of the stationary points. A scale factor of 0.9806 was used to obtain the ZPVEs from the calculated harmonic vibrational frequencies, while unscaled frequencies were used to obtain the thermal corrections to the enthalpy. The use of scale factors provides a means of accounting for systematic deviations between measured and computed frequency-dependent properties, and is an important consideration for the accurate description of reaction kinetics and thermochemistry [12]. Single-point energy calculations were performed using the BMK functional in conjunction with the 6-311 + G(3df,2p) basis set [13]. The BMK functional was recently developed by Boese and Martin and is accurate to approximately 10 kJ/mol for the calculation of reaction barriers. The good performance of BMK appears to hinge on the combination of a high percentage of Hartree–Fock exchange (42%), together with terms dependent on the kinetic energy density, resulting in a “back-correction” for excessive HF exchange in systems where this would be undesirable. The BMK functional was also found to be a method of choice in our level-of-theory study on the abstraction reaction in benzene [8], as it is an accurate computational method and yet affordable for systems of moderately large size, such as those studied in the present work. We applied TST to calculate the rate constants $k(T)$ [14–17]. The link with the macroscopic quantities found in the Arrhenius rate law is made by a linear fit of $\ln k(T)$ values, calculated for a range of temperatures, versus $1/T$. One refinement in our theoretical treatment comes from the observation that some of the low vibrational modes correspond to internal rotations rather than pure oscillations.

The standard harmonic oscillator (HO) model is known to be inappropriate for such modes and other approximations, such as the free rotor (FR) or hindered rotor (HR) model are advisable for the description of these modes [18]. For identification of internal rotations, one must analyze the low vibrational spectrum of the molecule. Due to steric

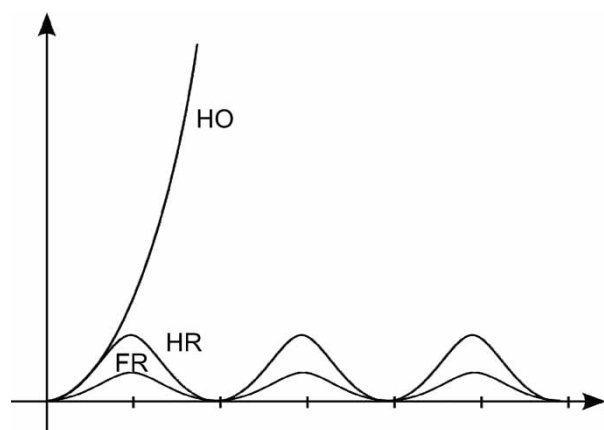


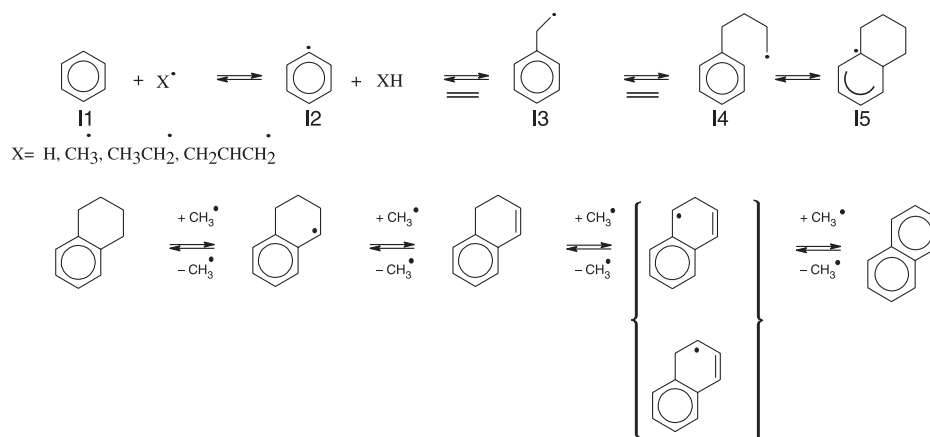
Figure 2. Potential within harmonic oscillator (HO), hindered rotor (HR) and free rotor (FR) model.

and electronic hindrance in the molecule, these rotations are opposed by a rotational potential. The choice of a particular description depends on the height of the rotational barrier and the temperature, as illustrated in figure 2. For low activated rotations the FR approach is used whereas for more hindered rotations the hindered rotor approach is applied. In a recent study of radical-addition reactions, we demonstrated the importance of correctly describing hindered internal rotations in order to obtain reliable partition functions [18]. Summarizing we use a mixed harmonic oscillator/free rotor (HO/FR) or mixed harmonic oscillator/hindered rotor (HO/HR) model, in which all the internal motions except for the internal rotations are approximated as independent harmonic oscillators.

3. Results and discussion

3.1 Reaction routes from benzene to naphthalene

In order to obtain microscopic insight into the importance of the various elementary reactions leading to coke, a reaction route starting from benzene and producing naphthalene is proposed, as shown in scheme 1.



Scheme 1. Reaction route starting from benzene to naphthalene.

At first instance the coke surface is approximated by one benzene ring. In the following section, the implications of this approximation will be validated on the rate determining steps of the coke network.

The reaction sequence is initiated by hydrogen abstractions from benzene with gas phase radicals creating radical surface species. In turn these radicals react further with unsaturated gas phase components. Ethene has been used as coke precursor, as it is the olefinic hydrocarbon with the largest concentration in the thermal cracking unit [19]. The initial hydrogen abstraction was studied both using a methyl and hydrogen radical. Earlier experimental work indicated that these radicals are very reactive in the coke formation during thermal cracking [20].

The reaction barriers at 0K, the frequency factors, activation barriers and the rate constants at three typical temperatures for coke formation are given in table 1 and for each reaction the transition state is shown in figure 3.

Rate constants of unimolecular reactions (e.g. cyclization reactions) and bimolecular reactions (e.g. hydrogen abstractions and addition reactions) cannot be directly compared as they have different units. To circumvent this problem modified rate constants are introduced for bimolecular reactions, by multiplication with the concentration of one the reactants:

$$\frac{dc_{\text{product}}}{dt} = k(T)c_Ac_B = k'(T)c_A \quad (1)$$

For the initial hydrogen abstraction, the reactant *B* is either the concentration of hydrogen or methyl radicals while for the addition reactions the concentration of ethene is used. Gas phase concentration profiles were obtained from a simulation program, which is based on a detailed network of elementary reactions, developed at the Laboratorium voor Petrochemische Techniek [21,22]. The reactor geometry and the operating conditions are taken for a typical ethane cracking unit. The process gas temperature profile as a function of the axial reactor coordinate is schematically shown in figure 4 and varies between 800 K at the reactor inlet to reach a coil outlet temperature of 1100 K. Typical concentrations of ethene and ethyne were

Table 1. Kinetic parameters of the elementary reactions of scheme 1. ΔE_0 and E_a are reported in kJ/mol, whereas A is in units of $\text{dm}^3/\text{mol}/\text{s}$ for bimolecular reactions and $1/\text{s}$ for unimolecular reactions. k and k' are the rate constant and modified rate constant as explained in the text. For the initial hydrogen abstraction with methyl and hydrogen Eckart tunneling was also incorporated.

Elementary reaction	ΔE_0 (kJ/mol)	A	E_a	$k(875\text{ K})$	$k'(875\text{ K})$	$k(1050\text{ K})$	$k'(1050\text{ K})$	$k(1075\text{ K})$	$k'(1075\text{ K})$
I1–I2 (with hydrogen)	62.53	$1.08\text{E} + 12$	79.62	$1.90\text{E} + 07$	$3.75\text{E}-05$	$1.18\text{E} + 08$	$1.15\text{E}-01$	$1.45\text{E} + 08$	$3.46\text{E}-01$
I1–I2 (with methyl)	71.00	$2.62\text{E} + 10$	80.9	$3.86\text{E} + 05$	$2.17\text{E}-06$	$2.46\text{E} + 06$	$1.34\text{E}-02$	$3.06\text{E} + 06$	$7.61\text{E}-02$
I2–I3	17.34	$8.92\text{E} + 09$	33.25	$9.21\text{E} + 07$	$2.32\text{E} + 01$	$1.97\text{E} + 08$	$6.20\text{E} + 05$	$2.16\text{E} + 08$	$1.27\text{E} + 06$
I3–I4	34.34	$6.91\text{E} + 09$	52.44	$5.10\text{E} + 06$	$1.28\text{E} + 00$	$1.70\text{E} + 07$	$5.32\text{E} + 04$	$1.95\text{E} + 07$	$1.15\text{E} + 05$
I4–I5	50.33	$9.90\text{E} + 08$	49.53	$1.09\text{E} + 06$	$1.09\text{E} + 06$	$3.39\text{E} + 06$	$3.39\text{E} + 06$	$3.87\text{E} + 06$	$3.87\text{E} + 06$
I5–I6 (with methyl)	66.33	$1.18\text{E} + 10$	80.54	$1.83\text{E} + 05$	$1.03\text{E}-06$	$1.16\text{E} + 06$	$6.27\text{E}-03$	$1.43\text{E} + 06$	$3.57\text{E}-02$
I5–I6	121.11	$6.52\text{E} + 13$	129.34	$1.23\text{E} + 06$	$1.23\text{E} + 06$	$2.38\text{E} + 07$	$2.38\text{E} + 07$	$3.36\text{E} + 07$	$3.36\text{E} + 07$
S1–S2	55.33	$1.29\text{E} + 10$	68.63	$1.03\text{E} + 06$	$5.77\text{E}-06$	$4.95\text{E} + 06$	$2.68\text{E}-02$	$5.94\text{E} + 06$	$1.48\text{E}-01$
S2–S3	64.33	$5.65\text{E} + 09$	78.90	$1.10\text{E} + 05$	$6.16\text{E}-07$	$6.68\text{E} + 05$	$3.62\text{E}-03$	$8.25\text{E} + 05$	$2.05\text{E}-02$
S3–S4	45.33	$4.60\text{E} + 09$	61.23	$1.01\text{E} + 06$	$5.69\text{E}-06$	$4.12\text{E} + 06$	$2.23\text{E}-02$	$4.85\text{E} + 06$	$1.21\text{E}-01$

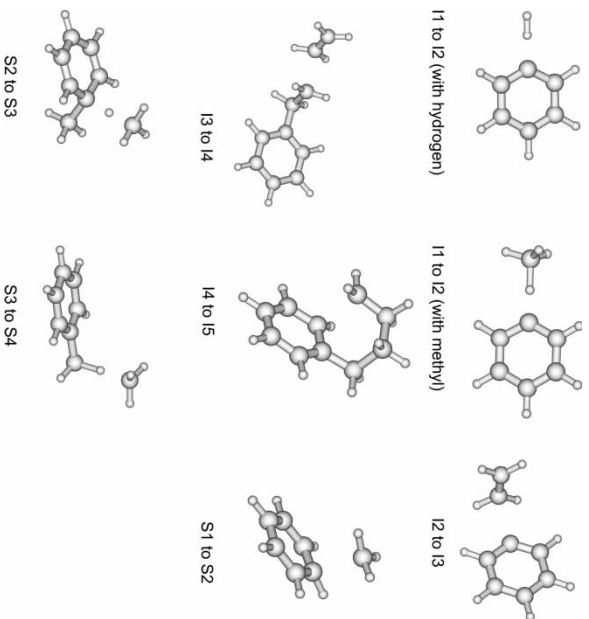


Figure 3. Transition states for the elementary reactions leading to cokes.

obtained at the reactor inlet, in the middle of the reactor length and at the outlet the reactor. These values are presented in table 2.

The modified rate constants are also tabulated in table 1 and are visualized in terms of temperature in figure 5. It is found that the initial hydrogen abstraction are relatively slow, due to the low concentration of the gas phase radicals. The individual rate constants however were found to be one of the highest in the total reaction network. This conclusion remains unaltered either considering methyl radicals or hydrogen radicals. The initially created radical surface species can further grow by means of various subsequent additions. The first addition of ethane or ethyne to the phenyl radical is characterized by a high rate constant. This can be explained by the reactivity of

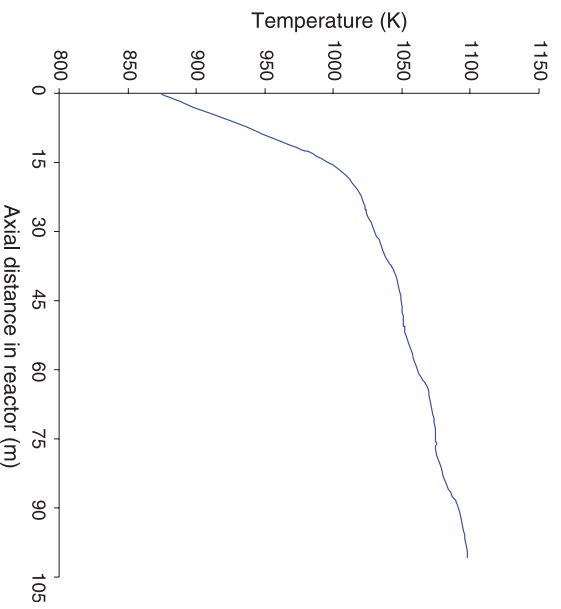


Figure 4. Temperature profile of the process gas along the reactor coil for typical ethane cracking conditions.

Table 2. Concentrations of ethene, the hydrogen and methyl radical at various axial reactor distances during ethane cracking. The concentrations are in units of k mol/dm^3 .

Axial distance	T	Ethene	H	CH_3
1.09 m	875	2.52E-07	1.98E-12	5.62E-12
44.02 m	1050	3.14E-03	9.80E-10	5.42E-09
100.96 m	1075	5.88E-03	2.38E-09	2.49E-08

the phenyl radical. The subsequent additions are slower whereas further cyclizations and dehydrogenation, proceed very fast. The dehydrogenation can proceed either by a hydrogen abstraction with a methyl radical or a β -scission with release of a hydrogen radical. The rate constants for both routes were calculated. The unimolecular reaction pathway, referred as I5–I5 in table 1 has a relatively high activation energy but also a much higher pre-exponential factor. Moreover due to the low concentration of methyl radicals, the β -scission is preferred. The final goal of this work should be the determination of the global coking rate. This requires the kinetic parameters of all elementary reaction steps as presented here, but also the concentration of all intermediate radicals. Therefore, the mass balances must be solved taking into account the pseudo-steady state assumption. This procedure was presented in the work of Wauters and Marin [1] but on basis of semi-empirical kinetic parameters. The prediction is the global coking rate with accurately determined kinetic parameters, as presented here, will be a topic of future research.

In scheme 1 the first step of the reaction network is the hydrogen abstraction creating a phenyl radical. Alternatively also a substitution reaction could take place with creation of toluene from which a hydrogen abstraction with methyl forms the benzyl radical.

The substitution reaction consists of two consecutive reactions: an addition of a gas-phase radical creating a hexadienyl radical (S1–S2) and release of the H atom with the formation of toluene (S2–S3). From that point benzylic type of radicals can be formed by abstraction by another gas phase radical. The kinetic parameters for these three reactions are given in table 3.

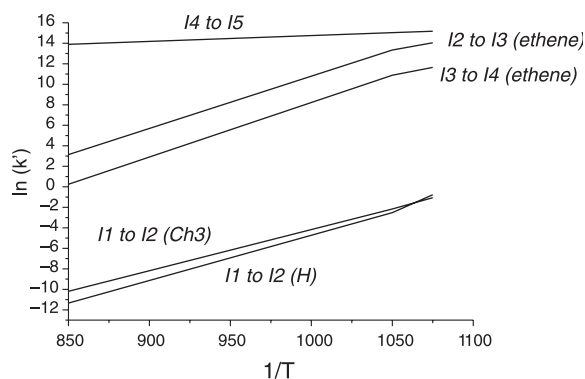


Figure 5. Modified rate constants for the elementary reactions leading to coke in the temperature interval 850–1100 K.

The hydrogen abstraction from toluene (S3–S4 in scheme 2) is substantially lower activated than the corresponding reaction starting from benzene. As benzylic type of radicals are much more stable than phenylic radicals, the activation barriers for the creation of the benzylic radicals is the lowest according to the Evans–Polanyi relation [23,24]. Also the first steps leading to toluene are all lower activated than the abstraction at benzene. When inspecting however the modified rate constants that also take into account the concentration of the gas phase radicals, these initial steps remain very slow.

Previous discussion reveals that the initial creation of surface species determines the global coking rate.

3.2 Influence of the coke matrix on the kinetics

The reaction network discussed in the previous section was based on the assumption that the coke surface could be approximated by only one benzene ring. It is however important to validate this approximation. Therefore, calculations were performed on larger polyaromatic compounds to establish the importance of the local environment of the active surface site in the coke formation. This is done for the initial hydrogen abstraction with the methyl radical creating a variety of possible aryl radicals.

Starting from a general polyaromatic (figure 6), a large number of possible reactive sites can be identified. It would be desirable to classify all possible aryl radicals of polyaromatic hydrocarbons (PAHs) into a limited set of groups, each characterized by a given reactivity. A measure of the chemical reactivity of a site at an aromatic cluster is the bond dissociation energy (BDE) of the corresponding C–H bond. BDEs of various aryl radicals formed from 13 PAHs, i.e. benzene, naphthalene, anthracene, tetracene, phenanthrene, benzo[c]phenanthrene, dibenzo[c,g]phenanthrene, benz[a]anthracene, dibenz[a,j]anthracene, coronene, benzo[a]naph[2,1-j]anthracene, benzo[a]phenanthr[2,1-j]-anthracene, benzo[ghi]perylene (figure 1) are studied, in order to determine the influence of the local polyaromatic environment on the C–H bond strength (figure 7).

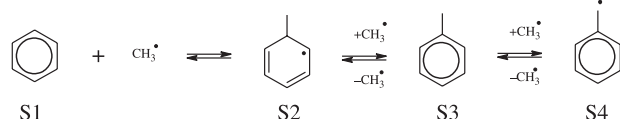
The BDE values segregate into six groups with different reactivity, and which can be related to the local structure around the site: benzene-like site (B sites), phenanthrene-like sites (P sites), dibenzophenanthrene-like sites (DBP sites), benzophenanthreneanthracene-like sites (BPA sites), benzophenanthrene-like sites (BP sites) and benznaphanthracene-like sites (BNA sites) (figure 8). The indication of the various sites is also indicated on the PAH of figure 6. More information about the classification can be found in reference [25]. The classification of PAHs into various groups was already suggested by Wang en Frenklach on the basis of semi-empirical calculations [26]. Only three classes were suggested due to the limited dataset that was considered. Other interesting references concerning BDEs of aryl radicals are the works of Chen *et al.*, Aihara *et al.* and Cioslowski *et al.* [27–29]. The latter

Table 3. Rate constants and pre-exponential factor in $\text{dm}^3 \text{mol}^{-1} \text{s}^{-1}$ and activation barrier in kJ mol^{-1} . All values were obtained using energies at the BMK/6-311 + G(3df,2p)//B3-LYP/6-311G(d,p) level and using a mixed HO/FR or HO/HR model, with inclusion of Eckart tunneling corrections.

Site	k_{700}	k_{900}	k_{1100}	E_a	A
B-1	2.55E + 04	5.12E + 05	3.97E + 06	80.9	2.62E + 10
N-1	1.45E + 04	2.99E + 05	2.36E + 06	81.6	1.69E + 10
N-2	1.74E + 04	3.53E + 05	2.76E + 06	81.1	1.86E + 10
A-1	7.36E + 03	1.64E + 05	1.35E + 06	83.6	1.20E + 10
A-2	1.34E + 04	2.76E + 05	2.18E + 06	81.6	1.55E + 10
A-3	1.99E + 04	3.96E + 05	3.05E + 06	80.7	1.96E + 10
T-1	7.62E + 03	1.68E + 05	1.39E + 06	83.4	1.20E + 10
T-2	1.78E + 04	3.62E + 05	2.83E + 06	81.2	1.94E + 10
T-3	2.15E + 04	4.25E + 05	3.26E + 06	80.4	2.04E + 10
PH-1	2.91E + 03	6.76E + 04	5.78E + 05	84.8	5.85E + 09
PH-2	8.62E + 03	1.73E + 05	1.34E + 06	80.8	8.78E + 09
PH-3	8.43E + 03	1.72E + 05	1.35E + 06	81.3	9.27E + 09
PH-4	6.39E + 03	1.30E + 05	1.01E + 06	81.2	6.89E + 09
PH-5	7.87E + 03	1.59E + 05	1.24E + 06	81.1	8.32E + 09
BPH-1	1.10E + 03	2.41E + 04	1.99E + 05	83.3	1.71E + 09
BPH-2	4.63E + 03	9.30E + 04	7.21E + 05	80.9	4.74E + 09
BPH-3	4.20E + 03	8.68E + 04	6.85E + 05	81.6	4.90E + 09
BPH-4	3.30E + 03	6.81E + 04	5.38E + 05	81.6	3.84E + 09
BPH-5	3.29E + 03	6.92E + 04	5.54E + 05	82.2	4.20E + 09
BPH-6	3.77E + 03	7.77E + 04	6.13E + 05	81.6	4.38E + 09
DBPH-1	9.96E + 02	2.14E + 04	1.74E + 05	82.8	1.41E + 09
DBPH-2	4.31E + 03	8.77E + 04	6.87E + 05	81.3	4.72E + 09
DBPH-3	3.48E + 03	7.40E + 04	5.96E + 05	82.4	4.64E + 09
DBPH-4	2.79E + 03	5.86E + 04	4.69E + 05	82.1	3.54E + 09
DBPH-5	2.78E + 03	5.97E + 04	4.84E + 05	82.7	3.88E + 09
DBPH-6	3.37E + 03	6.92E + 04	5.44E + 05	81.5	3.81E + 09
DBPH-7	2.72E + 03	5.90E + 04	4.80E + 05	82.9	3.93E + 09
BA-1	1.92E + 03	4.61E + 04	4.02E + 05	85.6	4.44E + 09
BA-2	1.51E + 02	4.53E + 03	4.57E + 04	91.6	9.71E + 08
BA-3	3.69E + 03	7.68E + 04	6.10E + 05	81.9	4.48E + 09
DBA-1	4.84E + 01	1.76E + 03	2.02E + 04	96.7	7.44E + 08
DBA-2	3.79E + 03	8.65E + 04	7.32E + 05	84.4	7.03E + 09
DBA-3	9.51E + 03	1.90E + 05	1.47E + 06	80.8	9.54E + 09
BNA-1	1.19E + 03	2.38E + 04	1.86E + 05	80.9	1.23E + 09
BNA-2	1.42E + 02	3.77E + 03	3.53E + 04	88.4	5.30E + 08
BNA-3	5.43E + 02	1.27E + 04	1.09E + 05	84.9	1.11E + 09
BPHA-1	4.59E + 02	1.12E + 04	9.83E + 04	86.0	1.13E + 09
BPHA-2	1.09E + 02	3.09 × 100	3.00E + 04	90.0	5.33E + 08
BPHA-3	1.30E + 03	2.72E + 04	2.18E + 05	82.1	1.64E + 09
C-1	3.63E + 04	7.70E + 05	6.18E + 06	82.3	4.77E + 10
PER-1	2.24E + 03	5.31E + 04	4.60E + 05	85.3	4.93E + 09
BPER-1	4.71E + 03	1.11E + 05	9.59E + 05	85.2	1.01E + 10

reference approximates the closest our work since the results are also based on *ab initio* techniques.

3.2.1 Kinetics of hydrogen abstraction by the methyl radical from PAHs. In this part attention is focused on the influence of the local environment of the C–H bond on the kinetics of corresponding abstraction reactions by a methyl radical. Rate constants $k(T)$, and corresponding activation energies E_a and pre-exponential factors A, for the reactions between the various PAHs and methyl radical were calculated at the BMK/6-311 + G(3df,2p)//B3-LYP/6-311G(d,p) level in the temperature interval of



Scheme 2. Radical substitution at the coke surface and further hydrogen abstraction with creation of a benzylic type of radical.

700–1100 K, which is relevant for the steam cracking and coke formation processes. Two refinements are taken into consideration in the calculations: the effect of tunneling corrections on the one hand, and a refined description of

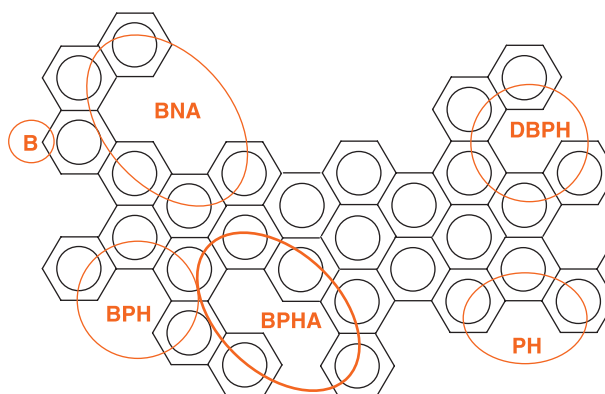


Figure 6. Representation of general PAH and classification into various sites.

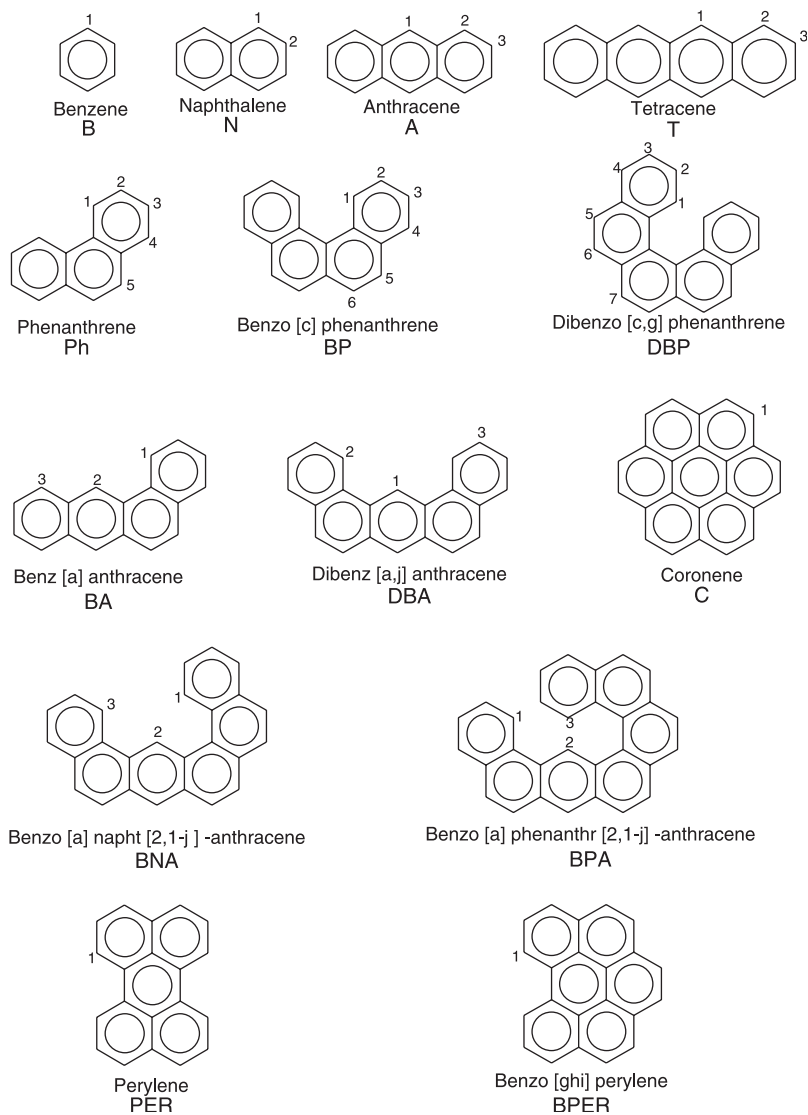


Figure 7. Polyaromatic hydrocarbons dataset. Distinct states at each PAH type are indicated and labeled.

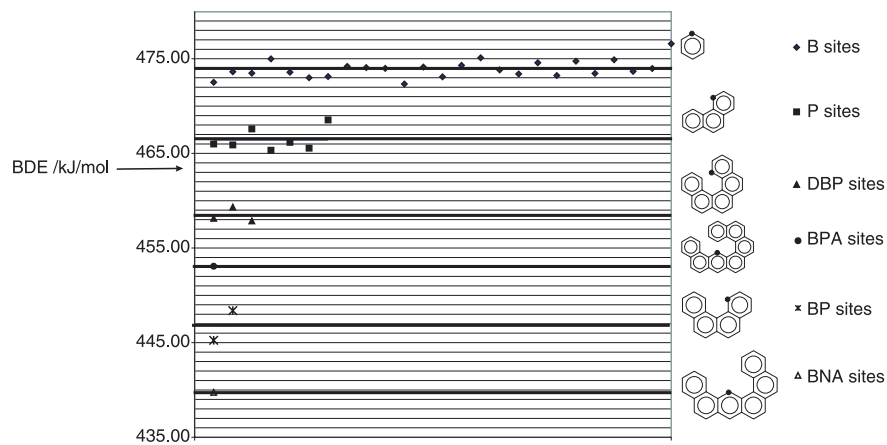


Figure 8. BDEs for various PAHs.

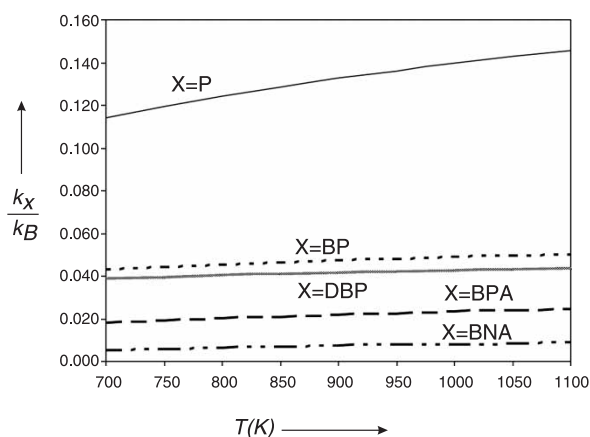


Figure 9. Rate constant for hydrogen abstractions with a methyl radical at site X, relative to the rate constant at the B site, as function of temperature.

the low-energy torsion of the methyl group in the TSs on the other. The calculated rate constants, activation energies and pre-exponential factors for the hydrogen abstractions are taken up in table 3.

The relative rates for hydrogen abstraction by a methyl radical at site X with respect to a benzene-like site are presented in figure 9. It can be concluded that abstraction is always preferred at less congested PAH molecules and most preferably at benzene-like sites. Earlier work also showed that even within a specific PAH, abstraction at B-like sites is always preferred over abstraction at more congested sites. For instance, for the various sites within the phenanthrene (P) molecule, the abstraction at the P-like site is more difficult than abstraction at the B-like sites [30].

4. Conclusions

In this paper, various elementary reaction steps important for coke formation during thermal cracking of hydrocarbons are studied. At first instance all elementary reaction steps of a reaction network starting from benzene and leading to naphthalene were studied in order to determine the slowest reaction steps of the network. The importance of all elementary reaction steps can only be validated when taking into account both rate constants for all elementary reactions and concentrations of gas-phase olefins and radicals. On basis of such analysis it can be concluded that the initial hydrogen abstraction is the slowest step of the reaction network. A competitive pathway for the initial hydrogen abstraction is the substitution reaction leading to toluene. The rates of these reactions are somewhat higher than for the hydrogen abstraction but due to the low concentration of methyl radicals in the reactor coils, also the substitution reaction is one of the slowest steps of the network. The coking rate is thus determined by the rate by which initial surface

species are created, either by direct hydrogen abstraction or by an initial substitution and subsequent hydrogen abstraction.

At second instance, the kinetic calculations were extended to larger polyaromatics, to investigate the influence of the local environment of the coke surface on the kinetic parameters. A classification for the reactivity of PAHs based on BDEs was proposed. Six different classes of C–H bonds could be identified. The influence of the local environment of the active site on the kinetics was investigated by studying a series of hydrogen abstraction reactions with the methyl radical. The latter reaction class was derived to determine the global coking rate of the reaction network. It was found that the rate constants can vary largely depending on the local structure of the polyaromatic surface. Moreover at typical temperatures encountered during cracking, hydrogen abstractions preferentially occur at the less congested PAH sites, such as benzene.

References

- [1] S. Wauters, G.B. Marin. Kinetic modeling of coke formation during steam cracking. *Ind. Eng. Chem. Res.*, **41**, 2379 (2002).
- [2] S. Wauters, G.B. Marin. Computer generation of a network of elementary steps for coke formation during the thermal cracking of hydrocarbons. *Chem. Eng. J.*, **82**, 267 (2001).
- [3] S. Wauters. Kinetics of coke formation during thermal cracking of hydrocarbons based on elementary reactions, PhD Thesis. Ghent University (2001).
- [4] M.F.S.G. Reyniers, G.F. Froment. Influence of metal-surface and sulfur addition on coke deposition in the thermal-cracking of hydrocarbons. *Ind. Eng. Chem. Res.*, **34**, 773 (1995).
- [5] M.J. Frisch, G.W. Trucks, H.B. Schlegel, G.E. Scuseria, M.A. Robb, J.R. Cheeseman, J.A. Montgomery Jr., T. Vreven, K.N. Kudin, J.C. Burant, J.M. Millam, S.S. Iyengar, J. Tomasi, V. Barone, B. Mennucci, M. Cossi, G. Scalmani, N. Rega, G.A. Petersson, H. Nakatsuji, M. Hada, M. Ehara, K. Toyota, R. Fukuda, J. Hasegawa, M. Ishida, T. Nakajima, Y. Honda, O. Kitao, H. Nakai, M. Klene, X. Li, J.E. Knox, H.P. Hratchian, J.B. Cross, V. Bakken, C. Adamo, J. Jaramillo, R. Gomperts, R.E. Stratmann, O. Yazyev, A.J. Austin, R. Cammi, C. Pomelli, J.W. Ochterski, P.Y. Ayala, K. Morokuma, G.A. Voth, P. Salvador, J.J. Dannenberg, V.G. Zakrzewski, S. Dapprich, A.D. Daniels, M.C. Strain, O. Farkas, D.K. Malick, A.D. Rabuck, K. Raghavachari, J.B. Foresman, J.V. Ortiz, Q. Cui, A.G. Baboul, S. Clifford, J. Cioslowski, B.B. Stefanov, G. Liu, A. Liashenko, P. Piskorz, I. Komaromi, R.L. Martin, D.J. Fox, T. Keith, M.A. Al-Laham, C.Y. Peng, A. Nanayakkara, M. Challacombe, P.M.W. Gill, B. Johnson, W. Chen, M.W. Wong, C. Gonzalez, J.A. Pople. *Gaussian 03, Revision B.03*, Gaussian, Inc., Wallingford CT (2004).
- [6] R.G. Parr, W. Yang. *Density-Functional Theory of Atoms and Molecules*, Oxford University Press, an example of a reference work (1989).
- [7] A.D. Becke. Density-functional thermochemistry. 3. The role of exact exchange. *J. Chem. Phys.*, **98**, 5648 (1993).
- [8] K. Hemelsoet, D. Moran, V. Van Speybroeck, M. Waroquier, L. Radom. An assessment of theoretical procedures for predicting the thermochemistry and kinetics of hydrogen abstraction by methyl radical from benzene. *J. Phys. Chem. A*, **110**, 8942 (2006).
- [9] L.A. Curtiss, K. Raghavachari, P.C. Redfern, J.A. Pople. Assessment of Gaussian-2 and density functional theories for the computation of enthalpies of formation. *J. Chem. Phys.*, **106**, 1063 (1997).
- [10] M.L. Coote. Reliable theoretical procedures for the calculation of electronic-structure information in hydrogen abstraction reactions. *J. Phys. Chem. A*, **108**, 3865 (2004).

- [11] B.J. Lynch, D.G. Truhlar. How well can hybrid density functional methods predict transition state geometries and barrier heights? *J. Phys. Chem. A*, **105**, 2936 (2001).
- [12] A.P. Scott, L. Radom. Harmonic vibrational frequencies: An evaluation of Hartree-Fock, Moller-Plesset, quadratic configuration interaction, density functional theory, and semiempirical scale factors. *J. Phys. Chem.*, **100**, 16502 (1996).
- [13] A.D. Boese, J.M.L. Martin. Development of density functionals for thermochemical kinetics. *J. Chem. Phys.*, **121**, 3405 (2004).
- [14] H. Eyring. *J. Chem. Phys.*, A more comprehensive treatment can be found in W.F.K. Wynne-Jones, H. Eyring, *J. Chem. Phys.* **3**, 492. This article is reproduced in full in M. H. Back, K. L. Laidler, *Selected readings in chemical kinetics*; Pergamon Oxford, 1967 **1935**(107).
- [15] K.J. Laidler. *Chemical Kinetics*, HarperCollins Publishers, Inc., (1987).
- [16] D.A. Mc Quarrie, J.D. Simon. *Physical Chemistry-A Molecular Approach*, University Science Books, Sausalito, California (1997).
- [17] P. Pechukas. *Dynamics of Molecular Collisions, Part B*, W.H. Miller (Ed.), Plenum Press, New York; (b) K. J. Laidler, M. C. King, *J. Phys. Chem.* **1983**, 87, 2657; (c) D. G. Truhlar, W. L. Hase, J. T. Hynes, *J. Phys. Chem.* **1983**, 87, 2664; (d) R. G. Gilbert, S. C. Smith, *Theory of Unimolecular and Recombination Reactions*, Blackwell: Oxford, 1990 (1976).
- [18] V. Van Speybroeck, D. Van Neck, M. Waroquier, S. Wauters, M. Saeys, G.B. Marin. Ab initio study of radical addition reactions: Addition of a primary ethylbenzene radical to ethene (I). *J. Phys. Chem. A*, **104**, 10939 (2000).
- [19] F.D. Kopinke, G. Zimmermann, S. Nowak. N the mechanism of coke formation in steam cracking – conclusions from results obtained by tracer experiments. *Carbon*, **26**, 117 (1988); (b) F.D. Kopinke, G. Zimmermann, G.C. Reyniers, G.F. Froment, Relative rates of coke formation from hydrocarbons in steam cracking of naphtha. 2. Paraffins, Naphthenes, Monoolefins, Diolefins, and Cycloolefins, and Acetylenes. *Ind. Eng. Chem. Res.*, **32**, 56 (1993); (c) F.D. Kopinke, G. Zimmermann, G.C. Reyniers, G.F. Froment, Relative rates of coke formation from hydrocarbons in steam cracking of naphtha. 3. Aromatic-hydrocarbons. *Ind. Eng. Chem. Res.*, **32**, 2620 (1993).
- [20] G.F. Froment. Fouling of heat transfer surfaces by coke formation in petrochemical reactors. In *Fouling of Heat Transfer Equipment*, E. Summerscales, J.G. Knudson (Eds.), Hemisphere Publ. Corp, (1981).
- [21] P.J. Clymans, G.F. Froment. Computer-generation of reaction paths and rate-equations in the thermal-cracking of normal and branched paraffins. *Comput. Chem. Eng.*, **8**, 137 (1984).
- [22] G.C. Reyniers, G.F. Froment, F.D. Kopinke, G. Zimmerman. Coke formation in the thermal-cracking of hydrocarbons. 4. Modeling of coke formation in naphtha cracking. *Ind. Eng. Chem. Res.*, **33**(11), 2584 (1994); (b) P.M. Plehiers, G.C. Reyniers, G.F. Froment, Simulation of the run length of an ethane cracking furnace. *Ind. Eng. Chem. Res.*, **29**, 636 (1990).
- [23] M.G. Evans. *Discuss. Faraday Soc.*, **2**, 271; M. G. Evans, J. Gergely, E. C. Seaman, *J. Polym. Sci.*, **1948**, 3, 866; M.G. Evans, M. Polanyi, *Trans. Faraday Soc.*, **34**, 11 (1938).
- [24] N.N. Semenov. *Some Problems in Chemical Kinetics and Reactivity*, Engl. Trans, pp. 29–33, Princeton Press, Princeton (1958).
- [25] V. Van Speybroeck, G.B. Marin, M. Waroquier. Hydrocarbon bond dissociation enthalpies: From substituted aromatics to polyaromatics. *Chem. Phys. Chem.*, **7**, 2205 (2006).
- [26] H. Wang, M. Frenklach. Enthalpies of formation of benzenoid aromatic-molecules and radicals. *J. Phys. Chem.*, **97**, 3867 (1993).
- [27] C.-C. Chen, J.W. Bozzelli. Structures, intramolecular rotation barriers, and thermochemical properties of methyl ethyl, methyl isopropyl, and methyl tert-butyl ethers and the corresponding radicals. *J. Phys. Chem. A*, **107**, 4531 (2003).
- [28] J. Aihara. Theoretical evidence for the presence of linear polyacenes in the interstellar-medium. *Bull. Chem. Soc. Jpn.*, **63**, 2781 (1990).
- [29] J. Cioslowski, G. Liu, M. Martinov, P. Piskorz, D. Moncrieff. Energetics and site specificity of the homolytic C-H bond cleavage in benzenoid hydrocarbons: An ab initio electronic structure study. *J. Am. Chem. Soc.*, **118**, 5261 (1996).
- [30] K. Hemelsoet, V. Van Speybroeck, D. Moran, G.B. Marin, L. Radom, M. Waroquier. Thermochemistry and kinetics of hydrogen abstraction by methyl radical from polycyclic aromatic hydrocarbons. *J. Phys. Chem. A*, **110** (50), 13624 (2006).